FLOW AND DISTRIBUTION OF WATER IN UNSATURATED, FRACTIONALLY-WET POROUS MEDIA SYSTEMS

ABU SALEM Z.[1] and WILLSON C.[2]

[1]Department of Civil Engineering and Infrastructure, Al Zaytoonah University of Jordan
[2]Department of Civil and Environmental Engineering, Louisiana State University
E-mail: zaydoun1@gmail.com

ABSTRACT

In recent years, interest in fluid flow and transport in the unsaturated zone has taken on increased importance because of the growing concern that the quality of the subsurface environment is being adversely affected by agricultural, industrial and municipal activities. The wettability properties (e.g., water repellency) of the porous media play an important role in determining fluid movement and ultimate distributions. Research studies (e.g., Bauters et al., 1998) have shown that preferential flow is likely to occur in water repellant soils resulting in spatial variability (over multiple scales) in the soil moisture.

The preferential flow paths can result in fast and deep infiltration of water and may impact solute and colloid/virus transport and plant growth. Numerical modeling of unsaturated flow through water-wet systems is complex due to the natural heterogeneities and number of constitutive relations (e.g., capillary pressure – water content, relative permeability) that must be determined when using conventional techniques such as Richard's equation.

This paper will results in better understanding of the flow and distribution of water in unsaturated, fractionally-wet (or water repellant soils) porous media systems where a series of capillary pressure – water content curves for drainage processes will be measured in the laboratory for a number of different media sizes/gradations and wettability conditions in order to develop the necessary constitutive relations.

Keywords: unsaturated zone, modeling, water repellant soils, drainage, imbibition

Introduction and Literature Review

Measurements and modeling of water flow and contaminant transport in soils and groundwater are generally macroscopic (spatial scale range of 1 cm to 1 m or larger); Fundamental mechanisms occur at microscopic scales (micrometer or smaller); Improved understanding and model predictions require microscopic approach. X-ray computed micro-tomography (CMT) provides three-dimensional nondestructive and noninvasive measurements of fluid saturation and concentration at the micro-scale Pore-scale measurements are being developed so that fundamental processes of flow & transport can be studied at pertinent micro-scale range, Figure 1.

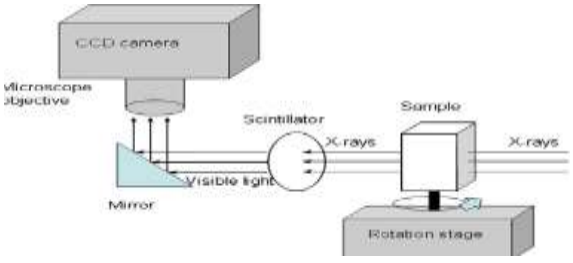

Figure 1: Conceptual diagram illustrating the principles of a typical conventional micro tomography setup.

The rate at which water infiltrates and drains within the subsurface following a rain or irrigation event and its distribution within the soil; have an impact on crop growth, evapotranspiration, and aquifer recharge. Hydrologists typically use drainage and imbibition relationships to describe the relationship between the capillary driving forces and the volumetric water content. These relationships, such as Van Genuchten and Brooks-Corey models, have been well-studied for wide variety of soils that are completely water wet (i.e., the water preferentially wets and soil particle compared to air). These models are presented as equations relate the volumetric water content with the capillary head acting on the water in the experiments resulting in water drainage (in drainage experiment) or wetting the porous media (in wetting experiment).

The Van Genuchten model equation of the water content for the drained soil is:

$$\theta = \theta_r + \left[\left(\theta_s - \theta_{ir} \right) / \left(1 + \left(\alpha_d \mathrm{h_c} \right)^{n_d} \right)^{m_d} \right]$$

where h_c is the capillary head, (θ) is the volumetric water content, (θ_{ir}) is the residual water content, (θ_s) is the fully saturated water content, α, m and n are fitting parameters to account for the air entry value and pore size distribution of the porous media, and in most cases m=1-1/n. Subscript $_d$ refers to the drainage process.

While the water content of the drained soil for Brooks-Corey model is:

$$\theta = \theta_r + \left[\left(\theta_s - \theta_{ir} \right) \left(\left(\mathrm{h_c} / h_b \right)^{-\lambda} \right) \right]$$

Where h_b is the bubbling pressure and λ is the soil characteristic index parameter.

Drainage experiment starts while the column is fully saturated, by reducing the water level in the end tube that connected to the column in multiple steps to allow the water from the sand to drain inside the tube. Imbibition experiment starts at the end of the drainage experiment by stepwise raising the water level at the end tube connected to the column to allow water to imbibe into the soil. The experimental setup is shown in Figure 2.

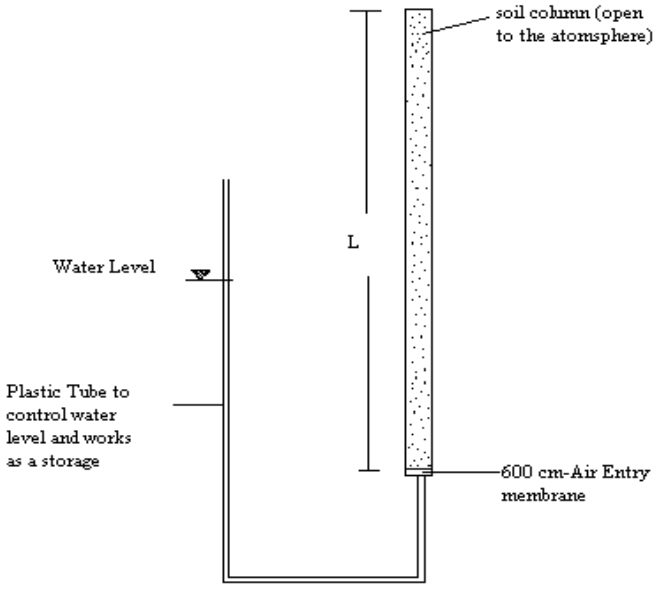

Figure 2: Experimental soil column apparatus used in the capillary pressure-water content experiments, with different sizes of columns and different wettabilities of porous media.

The difference in both models can be explained from the laboratory experiments, as shown in Figure 3, where the value for air entry pressure in the Brooks-Corey model has a definite number while at Van Genuchten equation it is smoothly variable.

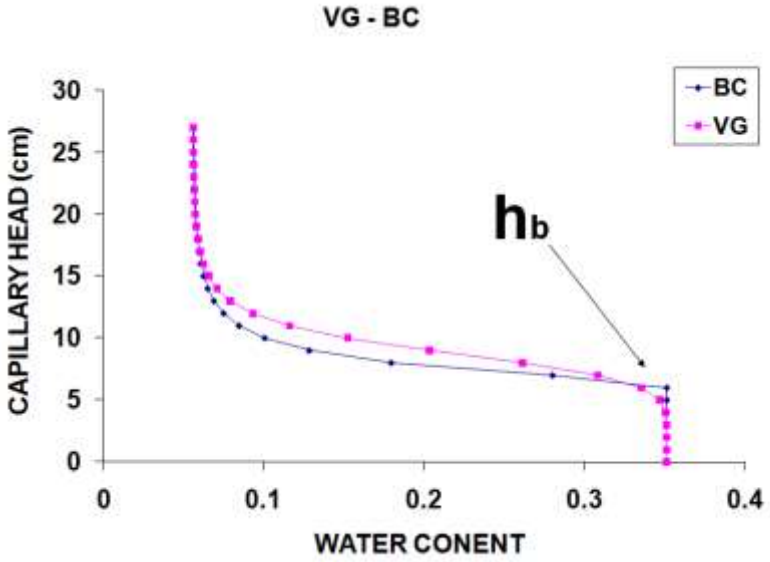

Figure 3: Van Genuchten and Brooks-Corey capillary pressure- water content for uniform sand.

The high-resolution images that conducting at the CAMD tomography beamline are directed at gaining insights in to the pore-scale processes and allow to quantitatively characterize the granular packing, the pore network structure (i.e., the pore bodies, throats, and connectivity), the distribution of the two fluids (e.g., water and air) within the pore space, and the correlation between the pore network structure and the fluid distribution.

Methodology

First, a series of capillary pressure – water content (hc-Θ) experiments were conducted in the laboratory in "large" columns (5 cm diameter, 20 cm in length) using standard procedures. Smaller aluminium columns (5 mm diameter, 10 cm in length) columns were used in the imaging experiments. Then, a series of capillary pressure – water content (hc-Θ) drainage experiments were conducted while the column was mounted in the CAMD tomography beamline hutch. At various points in the drainage experiments, the columns were imaged using a 35.3 keV monochromatic beam at 9 micron resolution.

The resulting 1 mm high tomography images allow us to qualitatively and quantitatively examine the pore-scale drainage. Water repellant sand was created by coating quartz sand with an organic chemical (OTS) that results in a water/air/solid contact angle of approximately 65 degrees. Fractionally-wet systems were created by packing the column with known fractions of the OTS-coated sand; in these experiments we used either 0% or 25% OTS-coated sand systems. Experimental procedures were identical in all columns.

Results and Conclusions

Results from the (hc-Θ) experiments in both the 0% and 25% OTS systems (Figure 4) were compared to literature values and to verify that the drainage processes are similar in the large and tomography columns. Attempts to perform drainage experiments in 50% OTS systems were unsuccessful due to the small size of the tomography columns and the increasingly complex nature of the drainage processes in highly water repellant systems. Of note is that as the system becomes more water repellant, the drainage curve shift lower resulting in more drainage at lower capillary pressure.

The results found from this work as in agreement with those found in the literature (e.g. Schroth et al. 1996, Bradford et al., 1995, and Seright et al. 2004) for the same type of sand with some differences in the values of the irreducible volumetric water content. This is mainly due to the wall effect where the representative elementary volume (REV) was not satisfied for this type of soil. It can be seen that all columns behaving the same in all the experiments. This is because of the consistency in preparing and performing the experiments and due to using the corrected equations to account for the column length.

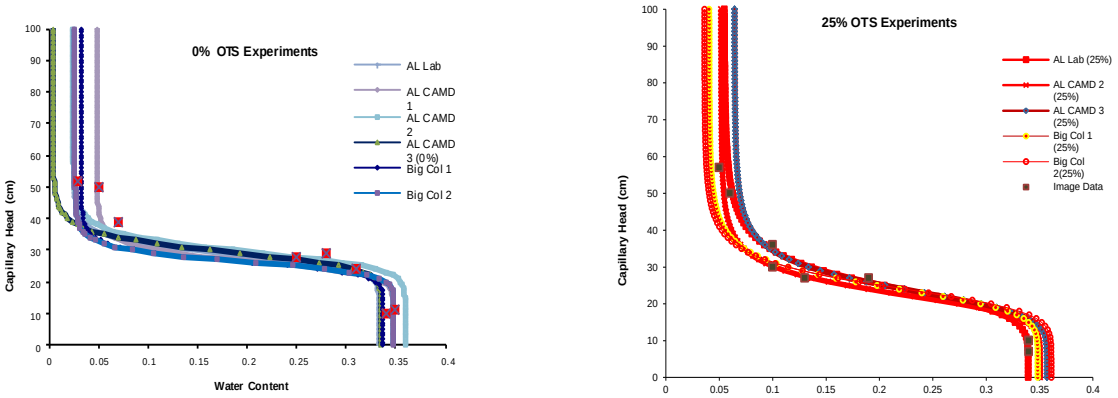

Figure 4: hc-Θ curves for 0% (top) and 25% (bottom) OTS-coated systems. AL refers to experiments conducted in tomography column and "Big Col" refers to experiments conducted in larger columns. The blocks symbols denote points along the drainage curves where imaged were collected.

Figure 5 is for the tomographic columns experiments with different percentage of fractional wettability soils (0%, 25% and 50% of OTS-wet treated soils). The soil hydraulic parameters were obtained using the Van Genuchten model.

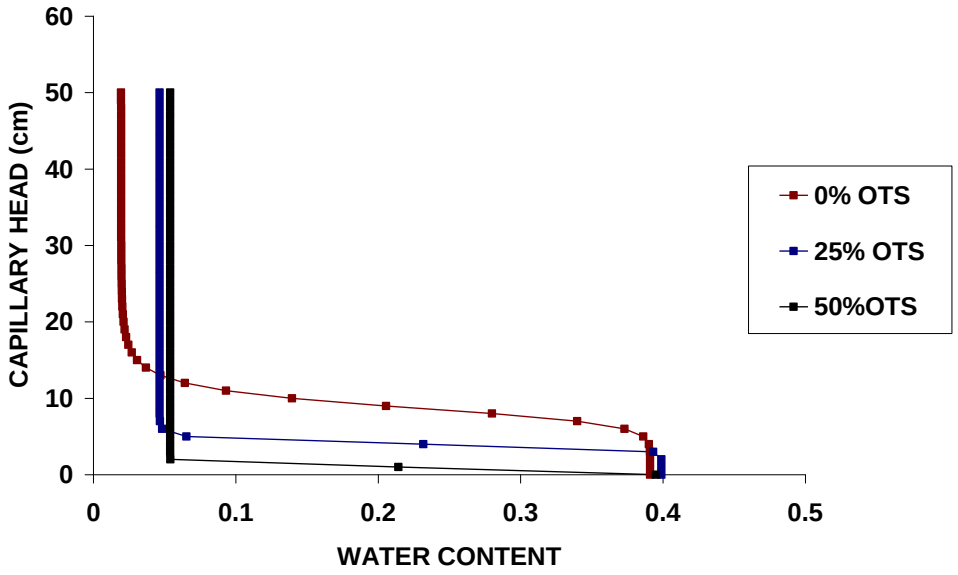

Figure 5: Saturation obtained for tomographic column experiments using Van Genuchten model and using (Accusand mesh 20/30).

An example of the drainage-wetting process for a 6 mm diameter sand pack, drained and re-saturated in steps to same sample-average saturation levels was done by Wildenschild and the following results were obtained from the CMT as the following (Figure 6).

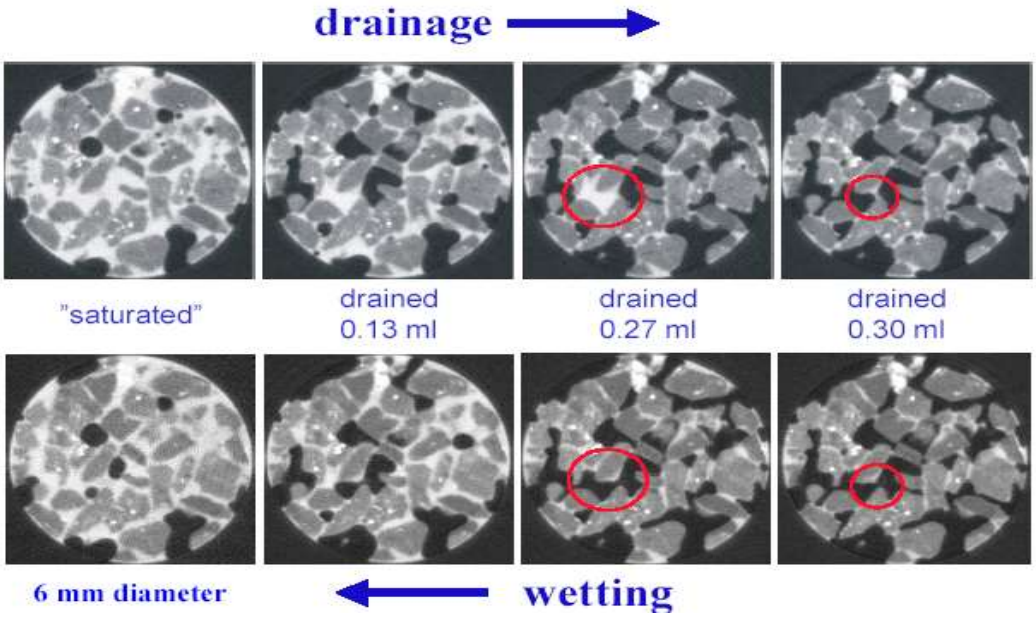

Figure 6: Horizontal slice through 3-dimensional images for the 6-mm diameter sand-pack drained and re-saturated in steps to same sample-average saturation levels. Wildenschild 2001.

Figure 7a is the scanned image for the Accusand 20/30 mesh for the fractional wettability experiment of 25% OTS above the iodide peak value in which air is one phase and the other phase is (solid and water). Figure 7b is the same as the previous scanned image but below the iodide peak value in which solid phase is one phase and the other phase is (water and air). The results of subtracting both segmented Figures 7a and 7b will give the water as one phase, the solid as second phase and the air as the third phase as shown in Figure 7c.

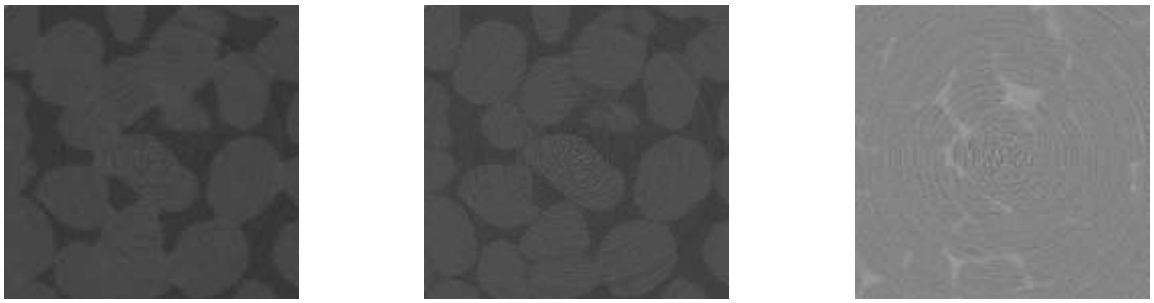

(a) (b) (c)

Figure 7: The scanned image for Ottawa sand for the fractional wettability of 25 % OTS (a) above the iodide peak, (b) below the iodide peak (c) the difference between a and b.

Figures 8a and b are the 3-dimensional image for the same section for the 25% OTS fractional wettability experimental column with slowly drainage process. The scanning images were taken above and below the iodide peak attenuation value respectively. Figure 8c is the segmented image for both the scanning images for the same experiment and the same section of the column showing the three different phases involved; air, water and solids

Representative images are shown in Figure 9. These figures show the solid (red), water (green) and air (phases) after the original images has been thresholded (i.e., the phase of each voxel has been uniquely identified). Of interest is that while the capillary pressure head conditions for both systems is approximately the same (28 cm for the 0% versus 27 cm for the 25%), the water content and distribution is different.

This work will results in better understanding of the flow and distribution of water in unsaturated, fractionally-wet (or water repellant soils) porous media systems. Current and future work is

directed at using algorithms to quantitatively analyzing the grain and pore structure, the water and air phase distribution properties, and the correlation between the pore structure and fluids.

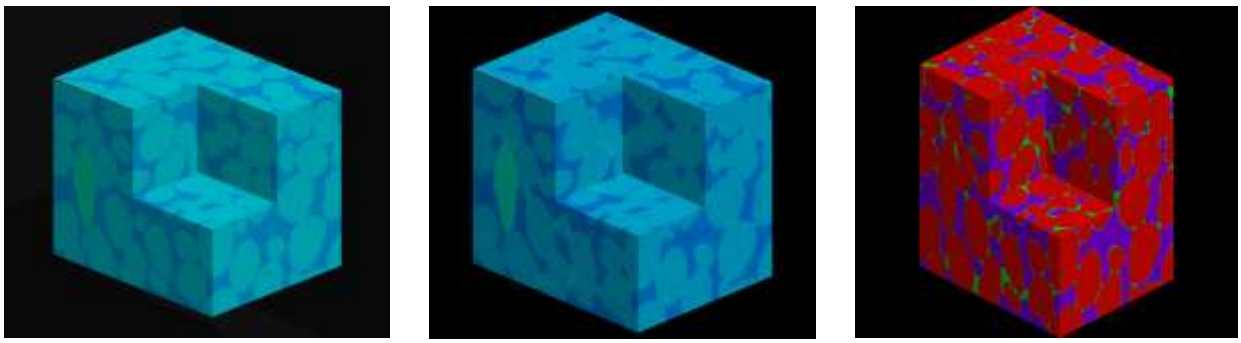

(a) (b) (c)

Figure 8: X-ray scanning image for 25% OTS fractional wettability with slowly drainage process experiment (a) above the iodide peak, (b) below the iodide peak and (c) the segmented image using the cutoff values T1=71 and T2=79 showing the three phases; air, water and solids.

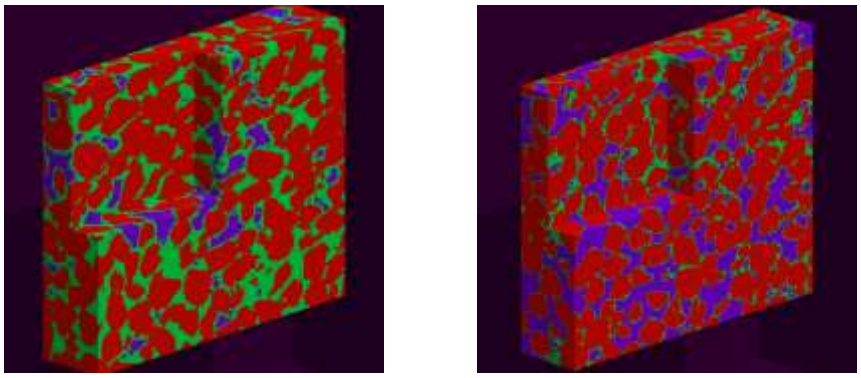

Figure 9: Thresholded images showing sand (red), water (green), and air (blue) in a 0% OTS system at 28 cm hc (left) and in a 25% OTS system at 27 cm hc (right).

REFERENCES

1. Bauters T., DiCarlo D, Steenhuis T., and Parlange J. (1998), Preferential Flow in Water Repellent Sands, Soil Sci. Soc. Am. Jor. 62: issue 5, 1185-1190.
2. Bradford S. and Feike J. L. (1995), Wettability Effect on Scaling Two- and Three-Fluid Capillary Pressure–Saturation Relations, Environmental Science and Technology. Vol. 29, no. 6.
3. Dullien, F.A. (1991), Characterization of Porous Media-Pore Level, Transport in Porous Media, 6, 581-606.
4. Royal H. Brooks and Arthur T. Corey, Properties of Porous MediaAffecting Fluid Flow, Journal of the Irrigation and Drainage Division, June 1966, Pages 61-88.
5. Schroth M. H. , S. J. Ahearn S. J. , Selker J. S. and Istok J. D. (1996), Characterization of Miller-Similar Silica Sands for laboratory Hydrologic Studies.
6. Seright R. S. and Lindquist B. (2004), X-Ray Computed Microtomography Studies of Disproportionate Permeability Reduction, SPE 89393.
7. Van Genuchten, M. Th. (1980), A Closed-Form Equation for Predicting the Hydraulic Conductivity of Unsaturated Soils. Soil Sci. Soc. Am. J. 44:892-898.
8. Van Genuchten M. (19800, A closed-form equation for predicting the hydraulic conductivity of unsaturated soils. Soil Sci. Soc. Am. J. 44:892-898.
9. Wildenschild D., Hopmans W., Rivers M. and Kent R. (2002), Quantitative Analysis of Flow Processes in A Sand Using Synchrotron Based X-Ray Microtomography, Vadose Zone Journal, 4:112-126.
10. Wildenschild D., Hopmans J. W., Rivers V., Rikard B., Christensen (2001), Using X-Ray Computed Tomography in Hydrology: Systems, Resolutions and Limitations.